Journal of Solid State Chemistry 221 (2015) 302–305

Contents lists available at ScienceDirect

Journal of Solid State Chemistry

journal homepage: www.elsevier.com/locate/jssc

Magnetic properties and adsorptive performance of manganese–zinc ferrites/activated carbon nanocomposites

B.B. Zhang [a], J.C. Xu [a], P.H. Xin [a], Y.B. Han [a], B. Hong [a], H.X. Jin [a], D.F. Jin [a], X.L. Peng [a], J. Li [a], J. Gong [a], H.L. Ge [a], Z.W. Zhu [a,b,*], X.Q. Wang [a,**]

[a] College of Materials Science and Engineering, China Jiliang University, Hangzhou 310018, China
[b] College of Mechanical and Electrical Engineering, China Jiliang University, Hangzhou 310018, China

ARTICLE INFO

Article history:
Received 31 July 2014
Received in revised form
10 October 2014
Accepted 14 October 2014
Available online 22 October 2014

Keywords:
Activated carbon
Nanocomposites
Magnetic properties
Adsorptive performance

ABSTRACT

Owing to the unique microstructure and high specific surface area, activated carbon (AC) could act as an excellent adsorbent for wastewater treatment and good carrier for functional materials. In this paper, manganese–zinc ferrites ($Mn_{0.5}Zn_{0.5}Fe_2O_4$: MZF) were anchored into AC by hydrothermal method, resulting in the excellent magnetic response for AC nanocomposites in wastewater treatment. All results demonstrated the magnetic nanoparticles presented a spinel phase structure and existed in the pores of AC. The saturation magnetization (*Ms*) of MZF/AC nanocomposites increased with the ferrites content, while the pore volume and specific surface area declined. The Sample-5 possessed the specific surface area of 1129 $m^2\,g^{-1}$ (close to 1243 $m^2\,g^{-1}$ of AC) and *Ms* of 3.96 emu g^{-1}. Furthermore, the adsorptive performance for organic dyes was studied and 99% methylene blue was adsorbed in 30 min. The magnetic AC nanocomposites could be separated easily from solution by magnetic separation technique.

1. Introduction

As the most common pollutants in wastewater, toxic organic dyes has been widely used for the dyeing of paper, bamboo, silk and so on [1,2]. The removal of organic dyes from wastewater has attracted more and more attention, and it was eager to develop the methods for the removal of organic dyes [3]. Adsorption was regarded as a popular method to remove pollutants from wastewater for the handleability and efficiency [4]. Owing to the high specific surface area and excellent chemical stability [5,6], activated carbon (AC) was acting as the most effective adsorbents for organic dyes in wastewater treatment. However, the conventional method of AC separation with filtration usually caused the blockage of filter and the loss of AC.

Recently magnetic separation technique was developed to overcome the disadvantage of filtration, in which the adsorbents should possess the excellent magnetic response [7,8]. With the implanting of magnetic medium into AC, the partial micropores were blocked, and the specific surface area must decrease to some extent. In order to obtain magnetic AC nanocomposites with both excellent adsorption capacity and magnetic response, AC should possess as high as specific surface area, additionally, the magnetic materials in AC nanocomposites are better to be higher saturation magnetization (*Ms*) and less concentration for keeping considerably good adsorption performance. Zhang et al. [9] prepared $CuFe_2O_4$/AC nanocomposites to adsorb and catalytically degrade acid orange II. Oliveira et al. [10] synthesized Fe_2O_3/AC magnetic nanocomposites for the adsorption of the volatile organic compounds such as chloroform, phenol, chlorobenzene and drimaren red dye from the aqueous solution. Yang et al. [11] synthesized magnetic Fe_3O_4/AC nanocomposites for the removal of methylene blue (MB) from aqueous solution. Faulconer et al. [12] synthesized magnetic γ-Fe_2O_3/AC nanocomposites by heterogeneous nucleation for aqueous Hg(II) removal and magnetic separation. The utilization of $MnFe_2O_4$ and $CuFe_2O_4$ ferrites for removing pollutants in wastewater has been mostly researched by Qu's group, which presented the excellent adsorptive properties and the highly effective recovery by magnetic separation technique [13]. Feng et al. [14] synthesized $NiFe_2O_4$/AC nanocomposites by the hydrothermal method for the adsorption and degradations of MB, rhodamine B and malachite green. Shao et al. [15] prepared $MnFe_2O_4$/AC nanocomposites by the chemical coprecipitation method as adsorbent for the removal of tetracycline from water or wastewater.

From the above works, the influence of magnetic oxides (such as γ-Fe_2O_3, Fe_3O_4, $NiFe_2O_4$, $MnFe_2O_4$, $CuFe_2O_4$ and so on) on the magnetic properties and adsorptive performance were discussed in detail. Among magnetic oxides, manganese–zinc ferrites

---

[*] Corresponding authors at: College of Materials Science and Engineering, China Jiliang University, Hangzhou 310018, China.
[**] Corresponding author.
E-mail addresses: zzw@cjlu.edu.cn (Z.W. Zhu), wxqnano@cjlu.edu.cn (X.Q. Wang).

http://dx.doi.org/10.1016/j.jssc.2014.10.020
0022-4596/© 2014 Elsevier Inc. All rights reserved.

($Mn_{0.5}Zn_{0.5}Fe_2O_4$: MZF) possessed the higher *Ms* and lower coercivity (*Hc*) than others [16,17]. As few as possible MZF could supply the sufficient magnetic response for magnetic separation, thus the magnetic AC nanocomposites possessed the higher specific surface area for the adsorption of organic dyes. In this work, MZF/AC nanocomposites were prepared via the hydrothermal method, and the microstructure, component and magnetic properties were characterized by X-ray diffraction (XRD), thermo gravimetric analysis (TGA) and differential scanning calorimetry (DSC), surface area and porosity analyzer (ASAP) and vibrating sample magnetometer (VSM). The influence of MZF content on the adsorptive performance for MB (a typical organic dye) was deduced and discussed in detail from the MB concentration after adsorption.

2. Experimental

2.1. Chemicals and reagents

Commercial carya peels based AC (100 mesh) was provided by Changnan Activated Carbon Co., LTD. (Zhejiang, China). All other chemicals, including zinc nitrate [$Zn(NO_3)_2 \cdot 6H_2O$],manganese nitrate [$Mn(NO_3)_2 \cdot 4H_2O$], ferric nitrate [$Fe(NO_3)_3 \cdot 9H_2O$], sodium hydroxide (NaOH) and methylene blue (MB), purchased from Hangzhou Chemical Co., LTD. (Zhejiang, China) were analytic grade. All solutions were prepared with deionized water.

2.2. Preparation of MZF/AC magnetic nanocomposites

A series of MZF/AC magnetic nanocomposites were prepared by a facile hydrothermal method, the detailed process was showed as the following. First, a certain amount of AC were added into 100 mL deionized water, which dissolved $Mn(NO_3)_2 \cdot 4H_2O$ (0.005 mol), $Zn(NO_3)_2 \cdot 6H_2O$ (0.005 mol) and $Fe(NO_3)_3 \cdot 9H_2O$ (0.01 mol) at room temperature. The mole ratio of MZF:AC was 1:25, 1:50, 1:100, 1:150 and 1:200 (named Sample-1, Sample-2, Sample-3, Sample-4 and Sample-5, respectively). After vigorous stirring for 24 h, the 9 mol L^{-1} NaOH solution was added dropwise to keep the pH value to 9.5. The mixture solution was laid into a reaction kettle and hydrothermal treated at 180 °C for 6 h. After cooling, the prepared magnetic composite was washed with distilled water repeatedly until the pH value reaches 7, which was then separated from water by an outer magnet and dried in the oven at 80 °C.

2.3. Characterization

The phase structure of MZF/AC nanocomposites were characterized by an XRD diffractometer (DX2700 China) with the Cu-$K\alpha$ radiation ($\lambda = 1.54051$ Å, step 0.02°) at 40 kV and 30 mA. Pyrolysis process (TGA/DSC) of the prepared nanocomposites was tested by a thermal balance instrument (SDT Q600, TA) in air with a heating rate of 5 °C min^{-1}. BET surface area, pore diameter, and pore volume were carried out by a surface analyzer (ASAP 2020 USA) with N_2 as the adsorbate at −196 °C. The magnetic properties of the prepared samples were measured by a vibrating sample magnetometer (VSM: LakeShore-7407) at room temperature up to 2 T.

2.4. Adsorption of methylene blue

Adsorption experiments for MB with AC and MZF/AC nanocomposites were carried out at room temperature for the different time. 0.05 g AC and MZF/AC nanocomposites were respectively put into glass vessels containing 50 mL MB solution (100 mg L^{-1}) to analyze the adsorption performance contrastively. The MB concentrations were determined by spectrophotometer (Shimadzu UV-3600) at 665 nm. The adsorption efficiency of MB was calculated with the equation [18]: $P(\%) = \left(((C_0 - C)/C_0)\right) \times 100$, where P was MB removal capacity (%), C_0 and C were the initial MB concentration and the MB concentration after adsorption with AC and MZF/AC nanocomposites.

3. Results and discussion

The crystalline structure of the as-prepared AC and MZF/AC nanocomposites were characterized by XRD. As shown in Fig. 1, all peaks were normalized according to the maximum peak. It is observed that two broad peaks are located at about $2\theta = 25°$ and 43° for AC, which indicates the existence of amorphous AC. With the implanting of MZF nanoparticles, the diffraction peaks of MZF with the cubic spinel phase structure (the space group *Fd*-3*m* (2 2 7) could be observed and marked with "•". And the diffraction intensity ratio of the main peak of MZF and AC increased with the MZF content. The unexpected diffraction peaks of α-Fe_2O_3 marked with "★" were also detected. This should be attributed to the unbalance into the pores of AC for the hydrated cation (Mn^{2+}, Zn^{2+} and Fe^{3+}) in the solution.

AC and MZF/AC nanocomposites were also measured by TGA in Fig. 2. The results indicated that the weight loss divided into two steps. The first soft slope of weight loss came out in the temperature range of 50–350 °C, which was attributed to the dehydration reaction below 100 °C and the desorption of gas adsorption at between 100 °C and 350 °C. The second steep slope of the weight loss observed at about 450 °C was due to oxidization of the amorphous carbon in the air. In this stage, the DSC curves (the

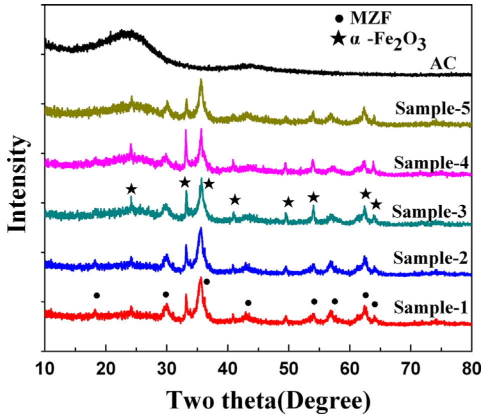

Fig. 1. The XRD patterns of AC and MZF/AC samples.

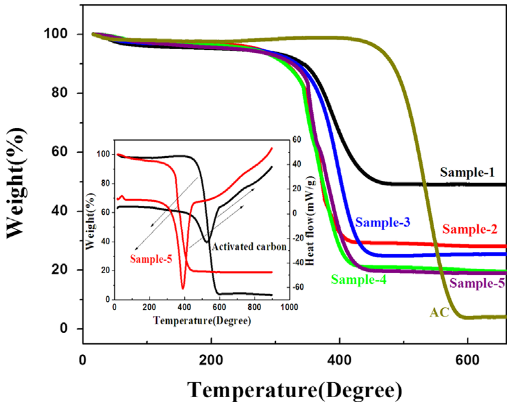

Fig. 2. TGA curves of AC and MZF/AC samples and TGA and DSC of AC and Sample-5.